CORRELATION BETWEEN THOR BrIC AND TBI RISK FROM FULL BODY HUMAN MODEL

Maika Katagiri
Ning Zhang
Jay Zhao
Jialou Hu
Mike Scavnicky
Bernd Cyliax
Ingo Mueller
Torsten Steiner
TAKATA Corporation
United States, Germany, Japan

Paper Number 15-0249

ABSTRACT

The Brain Injury Criteria (BrIC) was recently developed by using two human head models (SIMon and GHBMC) and ATD impact and crash test data. This study used a system simulation approach to further investigate correlations between BrIC from the THOR sled tests in the NHTSA Advanced Adaptive Restraint Program (AARP) and the human occupant traumatic brain injury (TBI) AIS 4+ risks estimated with a full body human model.

Eleven sled tests for the 50thpercentile male THOR Mod Kit dummy performed in AARP were selected as the basis for this analysis. The measured THOR BrIC values from these tests ranged from 0.49 to 1.89. For each of the THOR sled tests, a FE system model was built and the correlation was confirmed with the physical test data. The full body human model, a combination of the GHBMC head model and the in-house Takata human body model (TKHM), has been validated at component and full body levels. The THOR dummy model was then replaced with the full body human model in the system and the sled test simulations for the human under the same test conditions were conducted. The maximum principal strain (MPS) and the cumulative strain damage measure (CSDM) from the human head model were calculated from deformation of the brain tissue elements. The risks of AIS 4+ TBI injuries per the CSDM and MPS measures were compared with those estimated with BrIC from the THOR sled tests using paired student t-tests.

Overall, good agreement of the head, chest and pelvis translational accelerations and the head rotational velocities between the THOR dummy and the human body model were found for the full frontal sled cases. Differences between the two were observed for the head rotational velocities under the oblique sled test conditions. The results of additional simulations where an impactor struck laterally the face-jaw of the THOR, TKHM and GHBMC indicated that the THOR head-neck twisted more and faster than the human models, which could be a major cause of the inconsistency in the oblique cases.

Linear correlations between the THOR BrIC and the AIS 4+ TBI risk estimations from CSDM and MPS outputs of the human model were observed (with R^2 score of 0.81 for CSDM and R^2=0.85 for MPS). The TBI risks estimated from the THOR sled tests and the human model were similar in the full frontal, while the BrIC from the THOR sled tests overestimated the TBI risks.

INTRODUCTION

Great efforts have been made in the past decade to reduce death and injury in motor vehicle crashes (MVC). New FMVSS and NCAP test protocols have been implemented by the National Highway Traffic Safety Administration (NHTSA), and more advanced restraint system devices such as dual stage frontal airbags, curtain airbags, knee airbags, seatbelt pretensioners, seatbelt load limiters, etc. have been introduced into the vehicle fleet. Nevertheless, according to the Center for Disease Control and Prevention, prevalence for TBI has increased in the past decade, and more than 50% of TBI related deaths were due to MVC. Therefore, more work has been needed to reduce TBI related injuries and deaths associated with motor vehicle traffic accidents.

Takhounts et al. 2013 explained the possible root causes for TBI being among the most frequent injury and death related to MVC: the current regulated testing protocols may not represent real world crash scenarios associated with TBI injuries; the Anthropomorphic Test Device (ATDs) used in the lab tests may not represent the human responses to crash loadings; and the current injury assessment methods may not represent the injury mechanism with TBI at

the organ and tissue level. The industry has been working diligently to address this issue. To improve the regulated testing protocol, small overlap and oblique vehicle crash test configurations were extensively investigated by NHTSA and IIHS. The newly developed THOR dummy significantly improves bio-fidelity compared to the Hybrid-III dummy, which is the current test standard. The Brain Injury Criteria (BrIC), a head rotational velocity-based injury measure for TBI, was recently proposed [Takhounts et al. 2013] as a compliment to the existing translational acceleration-based HIC, which mainly acounts for contact-induced brain injury.

In development of BrIC, Takhaunts et al. used a series of linear impactor tests for the head-neck complex from the Hybrid III 50th male and 5th female dummies, THOR 50th male dummy, ES-2re, SID-IIs, WorldSID 50th Male and 5th Female, and 223 NCAP and frontal offset tests with 7 ATDs, in combination with simulation analysis using the two human head FE models (Simon and GHBMC), which were validated against various human brain response datasets, to develop correlation between BrIC for all ATDs and the human TBI risks estimation with the human head models. The head kinematics, including linear and angular accelerations measured from the dummy, were directly applied as the loading conditions to the human head FE models to calculate the brain tissue deformation. Such an approach for developing the TBI risks vs. BrIC relationship potentially over-looked or inaccurately estimated possible differences between the dummy-human kinematics responding to different crash conditions, and the dummy-human interactive forces with the restraint system (seatbelt and airbags), especially for the head-neck complex. These differences might significantly affect the TBI risk estimation with the human head models. To better understand and quantify the dummy-human kinematics difference, we were motivated to conduct further investigation at the system level using physical THOR sled test data and a reliable full body human model.

Two main tools were employed to conduct this study. First, FE models developed as part of the NHTSA-funded Advanced Adaptive Restraints Program (AARP) were utilized. In this research, the influence of multiple system variables on the baseline restraint system performance were investigated, such as the crash pulse severity in full frontal and oblique loading directions, different occupant sizes, positions and postures, and restraint configurations [Cyliax et al. 2015]. Dozens of AARP sled tests using the THOR Mod Kit dummy under different impact conditions were performed. For each of the baseline THOR sled tests, a sled system FE model was constructed and correlated. The THOR sled tests with the advanced adaptive restraint system (AARS) were simulated, and the AARS system models were verified by conducting sled tests. The second tool employed was an in-house mid-sized male human body FE model (TKHM) [Zhao et. al. 2007, Zhang et al. 2013].

The objectives of this study were:

1) To obtain a better understanding of the THOR 50thpercentile male dummy and human 50thpercentile male occupant kinematics and responses under the AARP sled test conditions, and how the kinematics differences between the human occupant and the ATD affect the brain injury prediction.
2) To investigate the correlation between the BrIC values resulting from the AARP sled test cases with the THOR dummy and the and the TBI risks estimated with the full body human model in the same AARP sled test cases.

METHODS

The current study took several steps to accomplish. First, a set of AARP sled tests for the driver male 50thpercentile THOR dummy using various sled test pulses and ATD positions/postures and the restraint configurations were performed and analyzed. Second, for each of the THOR test cases, a correlated driver sled system FE model was developed. Third, the THOR sled test model was replaced with a validated human full body model, and the sled test with the human model was simulated for the same test conditions. Finally, the human model results were analyzed to estimate the tissue level human brain injuries. Correlations between the measured BrIC from the AARP THOR sled tests and the CSDM or MPS based TBI risks from the whole human body models were investigated.

AARP THOR Sled Tests

For this study, eleven driver-side sled tests using the THOR Mod Kit dummy from the AARP were selected. In selecting the tests, the following considerations were made: 1) the measured THOR BrIC values, which were calculated using Eq. (1) [Takhounts et al. 2013], covered a wide range; 2) the corresponding sled system FE model correlated well to the corresponding sled test. Table 1 lists the selected driver THOR sled tests and the measured HIC and BrIC values, with the “soft” pulse representing a 35mph crash of an average mid-sized passenger car in the current fleet, the “hard pulse” representing a 35mph crash of a sub-compact car, 0 degree sled representing the full frontal crashes, and the left 15 degree angled sled simulating for the oblique crashes. In all the sled tests in Table 1, the THOR dummy was seated in the mid-track seat position, with a “normal” posture (as per the FMVSS-208 seating protocol), or a “forward leaning” posture. From the tests, the BrIC values ranged from 0.46 to 1.89, and the HIC ranged from 116 to 547.

$$BrIC = \sqrt{\left(\frac{\omega_x}{\omega_{xC}}\right)^2 + \left(\frac{\omega_y}{\omega_{yC}}\right)^2 + \left(\frac{\omega_z}{\omega_{zC}}\right)^2} \qquad \begin{matrix} \omega_{xC} = 66.25 \\ \omega_{yC} = 56.45 \\ \omega_{zC} = 42.87 \end{matrix} \qquad \textbf{(1)}$$

$$\omega_x, \omega_y, \omega_z: maxmum\ of\ absolute\ angular\ velocities$$

Table 1. AARP sled tests selected for this study (Seatbelt: SB, Driver Airbag: DAB, Curtain Airbag: CAB, Knee Airbag: KAB)

Test Number	Sled Pulse	Sled Angle [deg]	Driver posture	Restraint System	BrIC	HIC15
BDSJ0141	Soft	0 (Full-Frontal)	Normal	SB, DAB, KAB	0.59	232
BDSK0372	Soft		Normal	SB, DAB, KAB	0.46	185
BDSJ0179	Hard		Normal	SB, DAB, KAB	0.80	301
BDSK0066	Hard		Normal	SB, DAB, KAB	0.63	311
BDSK0108	Hard		Normal	SB, DAB, KAB	0.68	283
BDSK0297	Hard		Normal	SB, DAB, KAB	0.62	226
BDSJ0173	Soft		Forward leaning	SB, DAB, KAB	0.49	116
BDSJ0180	Hard	Left-15 (Oblique)	Normal	SB, DAB, KAB	1.74	400
BDSK0109	Hard		Normal	SB, DAB, KAB, CAB	1.54	547
BDSK0124	Hard		Normal	SB, DAB, KAB, CAB	1.89	326
BDSK0341	Hard		Normal	SB, DAB, KAB, CAB	1.13	237

AARP THOR Sled System Model

For each of the sled tests in Table 1, a FE system model was built with Ls-dyna 971 v6.1.2 (LSTC, Livermore, CA), and was validated at both the component level and the system level.
At the component level, all the restraint components used in the AARP driver system, including the baseline and adaptive driver airbags, knee airbag, curtain airbag, the baseline and adaptive seat belt, steering wheel and column were tested, and the FE models representing these components were validated with various impact tests. The THOR dummy model (V2.0beta, NHTSA) was updated and validated with the certification tests and the AARP sled tests [Zhao et al. 2015].
The validated component models were integrated into the AARP driver sled system models. For each of the driver THOR sled tests in Table 1, a system model was set up per the test configuration and the sled test simulation was conducted. The system model was then validated with the sled test data. Correlations were made for the dummy kinematics, the time-histories of the dummy measurements, and the injury measures between the test and the model. Quality of the correlations were accessed with the same methods and criteria developed for evaluation of the THOR Mod Kit dummy model system performance [Zhao et al. 2015]. Appendix-A (Figures A-1 through A-11) show the correlations of the accelerations of the head CG, chest CG, pelvis CG, and the head rotational velocities for all the cases in Table 1.

Full Body Human Model

The Takata Human Model (TKHM) version v5.3 was developed and used for this study. The model is a combination of the main body (excluding the head) of the TKHM version v4.3 and the same GHBMC (Global Human Body Model Consortium) head model v3.5 used in the BrIC study [Takhounts, 2013]. Prior to this study, the TKHM v4.3 model was extensively validated at component and full body levels [Zhao, 2007, Zhang, 2013], and the GHBMC head model [Mao, 2013] was correlated to PMHS intracranial pressure data [Nahum et al, 1977 and Trosseille et al 1992], brain motion tests [Hardy et al. 2001, 2007], and facial bone impact data [Nyquist et al. 1986, Allsop et al. 1988].
In this study, additional validations were made for the integrated neck-head assembly responses at both segment and full head-neck assembly levels to assure the biofidelity of the head-neck complex model.
At the cervical spine segment level, simulations were made for the motion segments of C1-C2 and C2-C3 in extension, flexion, lateral-bending, and torsion loadings at a maximum rotational speed of 0.00873 rad/sec

achieved at 36 msec. Figure B-1 (Appendix-B) shows the model predicted motion segment stiffness of C1-C2 and C2-C3 in extension, flexion, lateral-bending, and torsion compared to the test data [Ashton-Miller et al. 1997]. It is seen that the model predicted stiffness for the simulated loading cases were within the test data corridors.

At the neck-head assembly level, five PMHS test configurations [Wismans et al. 1986, Thunnissen et al. 1995, Davidsson et al. 1998, Hynd et al. 2007, Deng 1999] used for the GHBMC neck model validations were simulated with the updated head-neck assembly model. Figure B-2 (Appendix-B) shows the model predicted full head-neck complex responses to extension, flexion, lateral-bending, and torsion compared to the test data. It is seen that the model responses of these validation cases are within or close to the test data corridors or targets.

The integrated full body model v5.3 was further validated for the whole body responses in the PMHS sled tests performed at UVA [Kent et al. 2006]. The PMHS driver sled test for the test subjects #533, #544, #546 was simulated. Figure B-3 shows the correlation of the traces of histories of the head CG, T1, chest CG, and pelvis CG between the human body model and the test data. The human model kinematics responding to the sled test conditions was close to the PMHS in the test.

AARP Sled Tests Simulations with Full Body Human Model

Case by case the AARP sled models were updated by replacing the Thor dummy model with the full body human model. The same H-point and pelvis angle of THOR dummy positioning were used to position the human model. The head CG, knee centers, and ankle positions were further verified to have matched the two positions. The seat foam was fit using a positioning simulation, and the seat belts were re-routed across the human model torso. The contacts were defined between restraints, seat, environment and the human body. All the other system parameters for the THOR sled models were kept the same for the human sled model.

Sled simulations with the human body model were conducted for all corresponding THOR sled tests in Table 1. Occupant kinematics among the physical THOR sled test, the numerical THOR sled test, and the numerical sled test with the human body sled model were compared. The time-histories of head CG, T1, chest CG, and pelvis CG outputs were correlated.

Development of Correlation between THOR BrIC and Brain Tissue Criteria (MPS and CSDM)

From the human model sled test simulation results for each test case, the CSDM and MPS were calculated from the deformation of the brain tissue elements. The MPS and CSDM based risks of AIS 4+ TBI injuries ($P_{human,MPS}$, $P_{human,CSDM}$) were calculated according to Takhounts et al, 2013 by Eq. (2) and (3) respectively.

From the THOR sled test results, the BrIC based risks of AIS 4+ TBI injuries corresponding to the MPS and CSDM measures ($P_{THOR,MPS}$, $P_{THOR,CSDM}$) were calculated by Eq. (4) and (5) [Takhounts et al., 2013] respectively. Each pair of the risks ($P_{human,MPS}$ vs. $P_{THOR,MPS}$, and $P_{human,CSDM}$ vs. $P_{THOR,CSDM}$) were compared with linear curve regression and paired student t-tests using Excel Data Analysis ToolPak (Microsoft Office 2010, Redmond, WA).

$$P_{human,MPS}(AIS\ 4) = 1 - exp\left(-\frac{MPS}{1.010}\right)^{2.84} \quad \textbf{(2)}$$

$$P_{human,CSDM}(AIS\ 4) = 1 - exp\left(-\frac{CSDM}{0.600}\right)^{1.8} \quad \textbf{(3)}$$

$$P_{THOR,MPS}(AIS\ 4) = 1 - exp\left(-\frac{BrIC}{1.204}\right)^{2.84} \quad \textbf{(4)}$$

$$P_{THOR,CSDM}(AIS\ 4) = 1 - exp\left(-\frac{BrIC-0.523}{0.647}\right)^{1.8} \quad \textbf{(5)}$$

RESULTS

Kinematics Analysis

For all the cases in Table 1, the video camera views in the THOR tests and the screenshots of the animation in the full body human model simulations were compared. Furthermore, the correlations of the time histories of accelerations of the head CG, the chest CG, and the pelvis CG and the head rotational velocities (Appendix-A) were also processed for quantitative comparison of the kinematics. It was seen that in all the full frontal test cases, the kinematics of the THOR model were similar to the human model, while in all the oblique cases, the kinematics of the THOR and the human model were different. As two examples, Figure 1.a and Figure 1.b show the kinematics comparisons for the full frontal test case BDSJ0179 and the oblique case BDSK0124 respectively. Figure 2.a and Figure 2.b compare the head angular displacements between the THOR sled test and the human model sled simulation for the two cases BDSJ0179 and BDSK0124 respectively. Taking the oblique test case BDSK0124 as an example, until the head-airbag contact at about 60 ms, both the drivers moved forward and outboard to the left at about the same speed. After the contact, the THOR head and neck twisted more to the right (inboard) at a higher rotational velocity compared to the human model head.

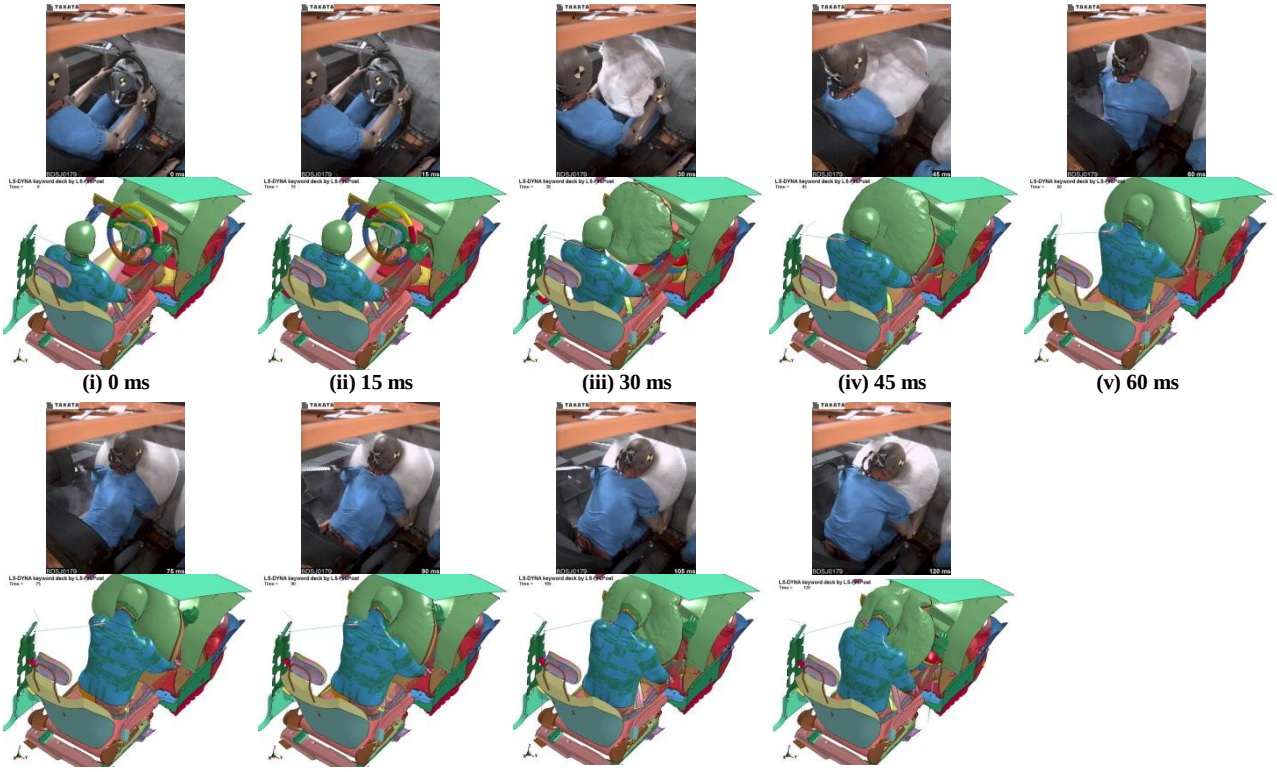

(i) 0 ms **(ii) 15 ms** **(iii) 30 ms** **(iv) 45 ms** **(v) 60 ms**

(vi) 75 ms **(vii) 90 ms** **(viii) 105 ms** **(ix) 120 ms**

(a) Full Frontal Hard Pulse (BDSJ0179)

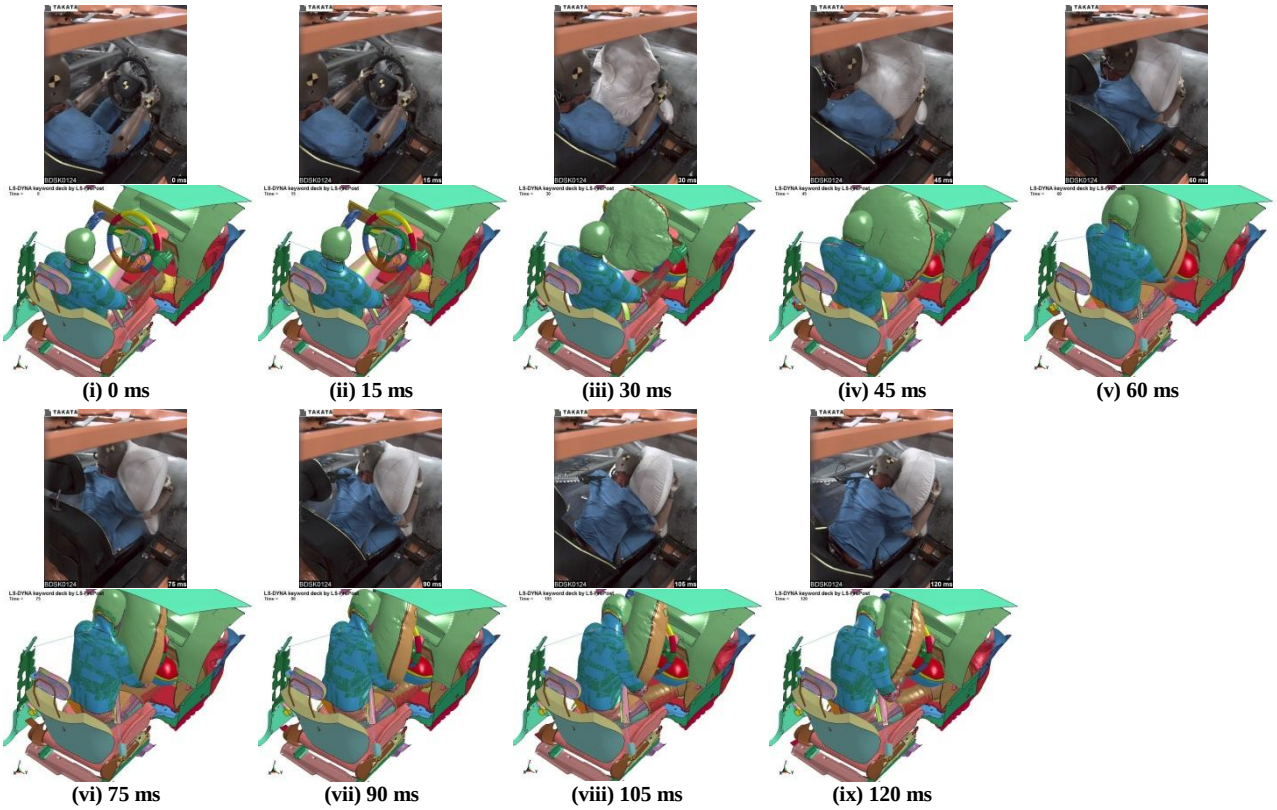

(i) 0 ms (ii) 15 ms (iii) 30 ms (iv) 45 ms (v) 60 ms

(vi) 75 ms (vii) 90 ms (viii) 105 ms (ix) 120 ms

(b) Oblique Hard Pulse (BDSK0124)

Figure 1. Comparison of the kinematics between the video camera views in the THOR sled test and the screenshots of animation in the same sled test with the full body human model

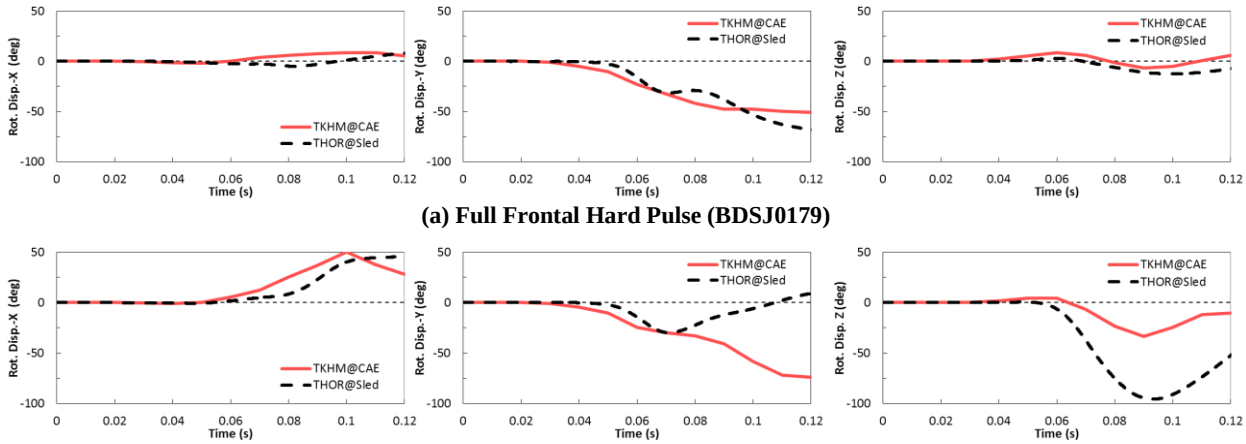

(a) Full Frontal Hard Pulse (BDSJ0179)

b) Oblique Hard Pulse (BDSK0124)

Figure 2. Comparison of the head angular displacements between the THOR sled test and the human model sled simulation. The dashed black curves were from the THOR, and the solid red lines were from the human model.

Figure 3.a and 3.b compare the head-airbag interaction forces of x-, y-, z- components between the THOR sled test simulation and the human model sled simulation for the two cases BDSJ0179 and BDSK0124 respectively. It was seen that in the full frontal case, the human head experienced the higher x- (longitudinal) force from the driver airbag than the THOR, while in the oblique case, the human head experienced the less y- (lateral) force than the THOR before 100 msec and got the higher force after that.

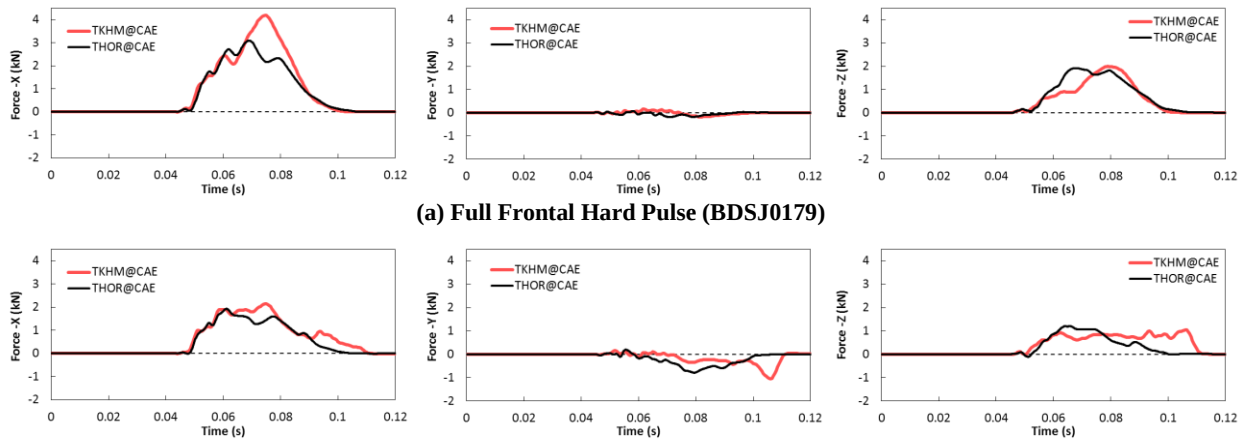

(a) Full Frontal Hard Pulse (BDSJ0179)

b) Oblique Hard Pulse (BDSK0124)

Figure 3. Comparison of the head-airbag contact forces between the THOR sled simulation and the human model sled simulation.

BrIC Values of THOR and Human Model

The BrIC obtained from the human model sled test simulations were compared to the THOR BrIC measured from the tests. Figure 4 depicts the correlation between these two groups of BrIC values. In Figure 4, all the THOR BrIC values of less than 0.8 were from the full frontal cases, and all the others above 0.8 were the oblique cases. It is seen that the BrIC from the human model were similar to the THOR in the full frontal group, but were much lower than the THOR in the oblique group.

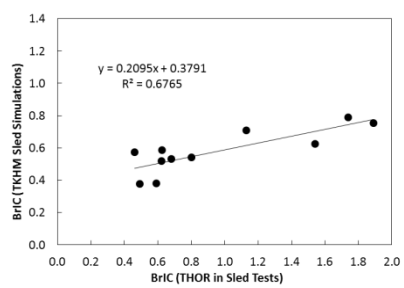

Figure 4. Comparison of BrIC between from the physical THOR sled tests and from the numerical sled tests with the full body human model

The bigger difference of the THOR BrIC values compared to the human head in the oblique cases was mainly due to the head Z-rotational velocity difference. Figure 5 compares the differences of the maximum of absolute head x-, y-, and z- angular velocities of the human model outputs subtracted by those of the THOR tests. It is seen that in the full frontal group such differences were small, while in the oblique cases, the z- angular velocities of the THOR were much higher than the human model, which were consistent with the kinematics difference analyzed above.

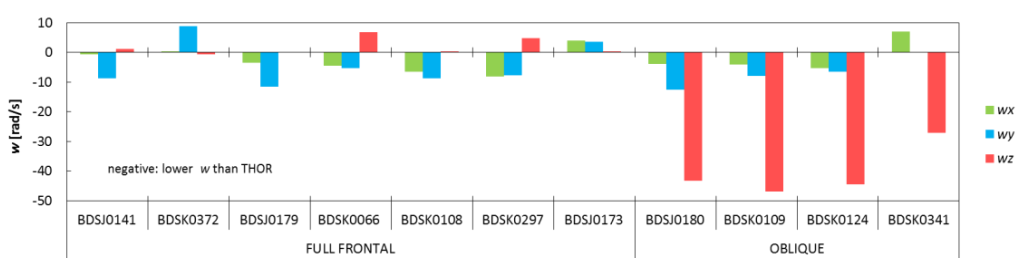

Figure 5. Differences of the maximum of absolute head angular velocities of the human model outputs subtracted by those of the THOR sled tests

AIS 4+ TBI Risks

Figure 6.a and 6.b respectively show the correlation between the pair of the TBI AIS 4+ risks ($P_{human,MPS}$ vs. $P_{THOR,MPS}$, and $P_{human,CSDM}$ vs. $P_{THOR,CSDM}$), where $P_{human,MPS}$ and $P_{THOR,MPS}$ are the MPS based risk from the human body model and the THOR BrIC measured from the sled tests respectively, and $P_{human,CSDM}$ and $P_{THOR,CSDM}$ are the CSDM based risk from the two respectively. Overall good correlations of each pair of these two were observed, with the correlation coefficient R^2 score of 0.85 for the MPS based risks and 0.81 for the CSDM based risks.

(a) MPS **(b) CSDM**

Figure 6. Comparison of AIS 4+ TBI risks between from the physical THOR sled tests and from the sled simulations with full body human model

DISCUSSIONS

Kinematics Difference between THOR and Human Model

The results of this study indicated that in all the oblique sled cases occupant kinematics differences in the head rotation between the human body model and the THOR were mainly due to the Z-rotation difference, One cause for such a difference was due to the less y- (lateral) airbag force applied to the human head than that to the THOR, as shown in Figure 3.b. Another cause could be the occupant head-neck models' torsional response to the impacts. To quantify the occupant head-neck models' torsional characteristics, additional numerical simulations for the quasi-static and dynamic loadings were performed for both the THOR and the human models.

The quasi-static loading cases per the Duke University study [Parent, 2015] were set up for the THOR Mod Kit head-neck assembly model, the human head-neck model (TKHMv5.3), and the GHBMC head-neck model (GHBMCv4.0), respectively, where the GHBMC head-neck model was taken as a reference for the comparison. Figure 7.a shows the simulation results of the torsional response of the THOR model and the two human models (TKHMv5.3 & GHBMCv4.0), compared to the Duke University PMHS tests data set [Parent, 2015]. It is seen that the torsional moments of T1 at the rotation angle of 63 degree of the THOR model, TKHMv5.3 and GHBMCv4.0 were in the corridors of the tests. The two human models' responses were very close and they all were lower than that of the THOR. The nonlinearities of the torsional stiffness were different between the dummy and human models. While the rotational moment at T1 of THOR increases almost linearly with the head rotation, the T1 moments of the human models were lower at the early stage of the rotation and increased nonlinearly.

Virtual linear impactor tests were set up for the THOR head-neck assembly model, the human head-neck model (TKHMv5.3), and the GHBMC head-neck model (GHBMCv4.0) respectively, in which a rigid cylinder with 43 mm diameter and a 5 kg mass laterally impacted the jaw of the head at an impact speed of 5 m/s. The T1 and below of each of the three head-neck assembly models in the test setup were constrained as fixed. Figure 6.b shows the simulation results of the torsional responses of the THOR model and the two human models to such an impact condition. Notably, the THOR rotational response (velocity and displacement) was approximately twice that of the human models under the same dynamic loading. These studies suggested that although the torsional stiffness of the human head-neck models was lower than the THOR under quasi-static loading, under dynamic loading, the THOR head-neck rotated more easily compared to the human model. Such

torsional characteristic differences between the THOR and the human head-neck could be a major cause of the occupant kinematics differences observed in the oblique sled cases.
Currently there is no published PMHS test data in this simulated dynamic loading. The simulated human model behaviors could be validated if such test data were available.

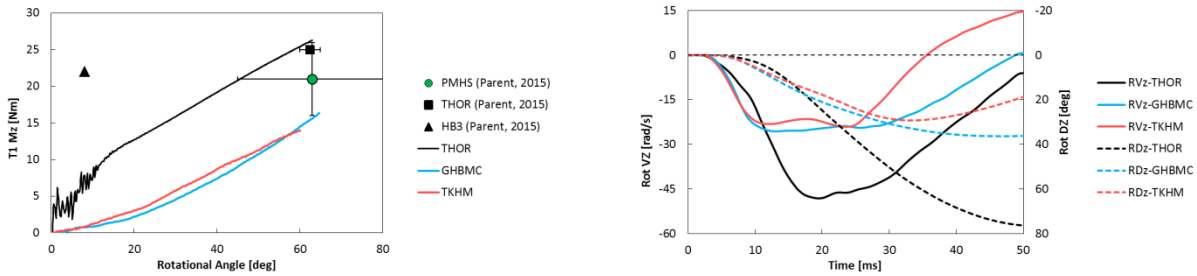

(a) Quasi-Static loading **(b) Dynamic impact**

Figure 7. Torsional responses of the THOR model, and the human models (TKHM & GHBMC) to the quasi-static and dynamic loadings

AIS 4+ TBI Risk Estimation Difference between THOR and Human Model

This study indicated that in all the full frontal sled test cases, the TBI 4+ risks estimated from Takhounts' risk function with the THOR BrIC from the sled tests were close to the MPS or CSDM based TBI 4+ risks from the human model. However, in all the oblique sled test cases, the THOR BrIC derived TBI 4+ risks were higher than those from the human model, which could be mainly due to the head-neck torsional characteristic difference discussed in the prior section.

Limitations of this Study

This study used a system simulation approach which requires high quality validated sled test models for the THOR as well as for the human body. In this study, the THOR sled models for all the test cases were well or fairly correlated with the test data. However, the corresponding human sled test models were not validated directly with PMHS sled tests since such data do not exist. The calculated CSDM and MPS values from the human model, which affect significantly the TBI injury risks outcomes, could be further verified.
This study observed significant head-neck torsional kinematic differences between the THOR and the human model in all the oblique sled test cases. The simulated face-jaw linear impactor tests for the THOR and the PMHS indicated that the THOR-human head-neck torsional characteristic differences under the dynamic impact condition could be a major cause. Compared to the THOR, the human head-neck has a lower torsional stiffness under quasi-static loading, exhibits a stiffer torsional response compared to the THOR under dynamic loading. These findings need verification to corresponding PMHS tests using the same face-jaw linear impactor test protocol.
Finally, this study used a relatively small sample size. More data points could provide further insight into the BrIC response with the THOR ATD.

CONCLUSIONS

A systematic method to use THOR sled tests and a full body human model to assess TBI risks was developed. This study confirmed that the BrIC from the THOR sled tests is a statistically significant indicator or measure for AIS 4+ TBI risk.
In the full frontal sled test cases, the occupant kinematics and the TBI 4+ injury risks between the THOR and the human model were similar.
In the oblique sled test cases, the BrIC and the AIS 4+ TBI injury risk from the THOR were higher than those estimated from the human model, which indicates the TBI risk in oblique crash scenarios using THOR could be over-estimated. This difference is possibly due to the observed difference of the head-neck rotational responses under dynamic torsional impact between the THOR and the human model. The dynamic impactor simulations indicate the human model head-neck exhibits a stiffer torsional response compared to the THOR.

ACKNOWLEDGEMENTS

The AARP project was funded by NHTSA Contract #DTNH22-12-C-00266. The authors greatly appreciate the support from NHTSA, especially James Saunders, Stephen Summers, and Dan Parent.

REFERENCES

Allsop, DL., Warner, CY., Wille, MG., Schneider, DC., Nahum, AM., 1988, "Facial Impact Response – A Comparison of the Hybrid III Dummy and Human Cadaver", In Proc. 32nd Stapp Car Crash Conference, SAE Paper No. 881719.

Ashton-Miller JA., and Schultz, AB. 1997. "Biomechanics of the Human Spine", Basic Orthopaedic Biomechanics, 2nd ed.

Cyliax, B., Scavnicky, M., Mueller, I., Zhao, J., and Aoki, H. 2015. "Advanced Adaptive Restraints Program Individualization of Occupant Safety Systems", SAE 2015 Government/Industry Meeting, Washington, DC.

Davidsson, J., Deutscher, C., Hell, W., Linder, A., Lovsund, P., Svensson, M., et al., 1998, "Human Volunteer Kinematics in Rear-end Sled Collisions", In Proc. IRCOBI conference, 289-301

Deng, B., 1999 "Kinematics of human cadaver cervical spine during low speed rear end impacts", PhD Thesis, Wayne State University.

Hardy, WN., Foster, C., Mason, M., Yang, K., King, A., Tashman, S., 2001, "Investigation of Head Injury Mechanisms Using Neutral Density Technology and High-speed Biplanar X-ray", Stapp Car Crash Journal 45: 337-368.

Hardy, WN., Mason, MJ., Foster CD., Shah, CS., Kopacz, JM, Yang, K, King, A, Bishop, J., Bey, M., Anderst, W., Tashman, S., 2007, "A Study of the Response of the Human Cadaver Head to Impact", Stapp Car Crash Journal 51: 17-80.

Hynd, D, Svensson, M, Trosseille, X, van Ratingen, M., and Davidsson, J., 2007, "Dummy Requirements and Injury Criteria for a Low-speed Rear Impact Whiplash Dummy", European Enhanced Vehicle-Safety Committee, EEVC WG12 #505A.

Kent, R., Forman, J., et al., 2006, "Whole-body Kinematic and Dynamic Response of Restrained PMHS in Frontal Sled Tests", Stapp Car Crash Journal 50: 299-336.

Mao, H., Zhang, L., Jiang, B., et al., 2013, "Development of a Finite Element Human Head model Validated with Forty Nine Loading Cases from Experimental and Real World Impacts", J Biomech Eng. 135(11), Paper No: BIO-12-1302.

Nahum, AM., Smith, R., and Ward, CC., 1977, "Intracranial Pressure Dynamics During Head Impact", In Proc. 21st Stapp Car Crash Conference, SAE Paper No. 770922.

Nyquist, GW., Cavanaugh, JM., Goldberg, SJ, King, A., 1986, "Facial Impact Tolerance and Response", In Proc. 30th Stapp Car Crash Conference", SAE Paper No. 861896.

Parent, D., 2015, "NHTSA THOR Update", THOR Public Meeting, Washington, DC.

Takhounts, E., Craig, JC., Moorhouse, K., and McFadden, J., 2013, "Development of Brain injury Criteria (BrIC)", Stapp Car Crash Journal 57: 343-266.

Thunnissen, J., Wismans, J., Ewing, C., and Thomas, D., 1995, "Human Volunteer Head-Neck Response in Frontal Flexion: A New Analysis", SAE Paper No. 952721.

Trosseille, X., et al., 1992, "Development of a F.E.M. of the Human Head According to a Specific Test Protocol, In Proc. 36th Stapp Car Crash Conference, SAE Paper No. 922527.

Wismans, V., Oorschot, H., and Woltring, H., 1986, "Omni-Directional Human Head-Neck Response" SAE Paper No. 861893.

Zhang, N., Katagiri, M., and Zhao, J. 2014. "TBI Risk Assessment with AARP THOR Sled Tests and a Full Body Human Model." The 42th International Workshop on Human Subjects for Biomechanical Research.

Zhao, J., Zhang, N., and Hu J. 2015. "Implementation of THOR FE Model in AARP Project", NHTSA Public Meeting Concerning Test Device for Human Occupant Restraint, Washington, DC.

Zhao, J., Narwani, G. 2007. "Biomechanical Analysis of Hard Tissue Responses and Injuries with Finite Element Full Human Body Model." ESV 07-0354.

APPENDIX A: AARP Sled Models Correlations

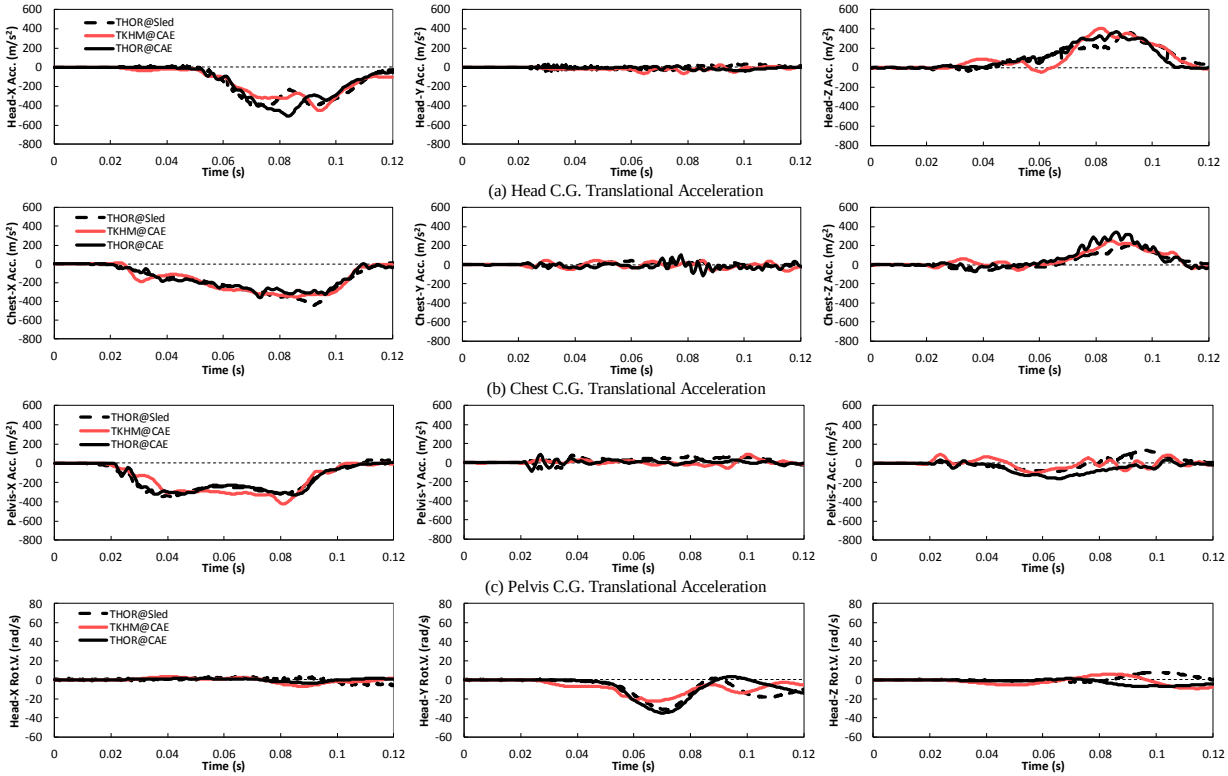

(a) Head C.G. Translational Acceleration

(b) Chest C.G. Translational Acceleration

(c) Pelvis C.G. Translational Acceleration

(d) Head C.G. Rotational Velocity

Figure A-1. Full Frontal Soft Pulse (BDSJ0141)

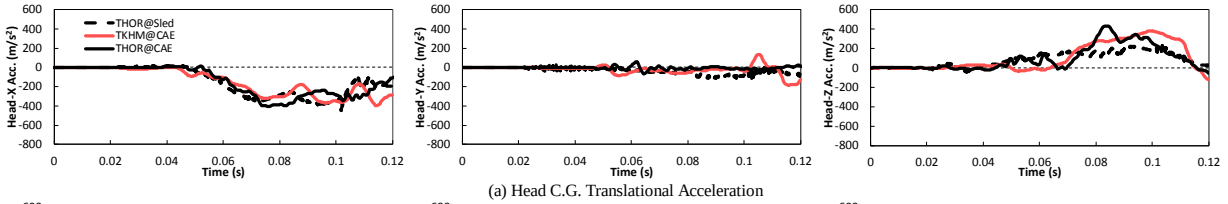

(a) Head C.G. Translational Acceleration

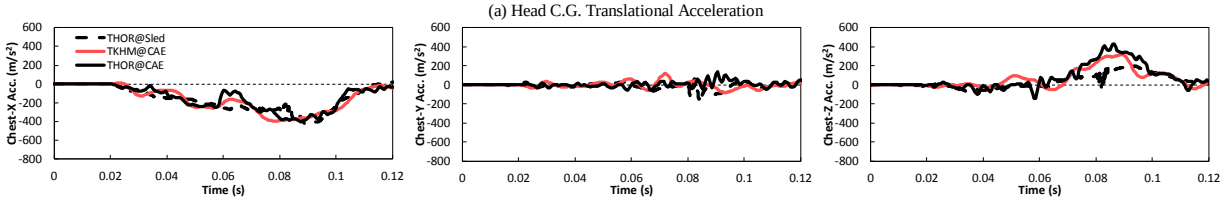

(b) Chest C.G. Translational Acceleration

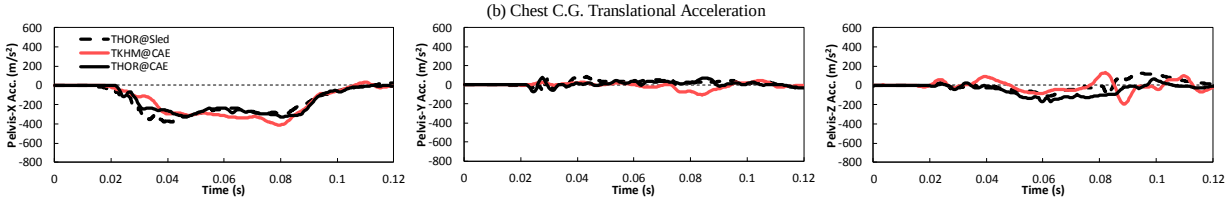

(c) Pelvis C.G. Translational Acceleration

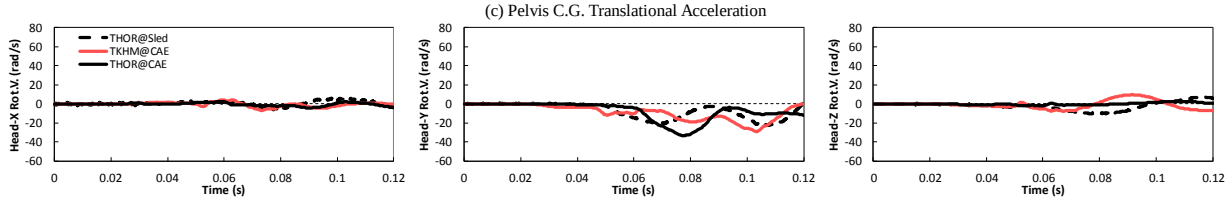

(d) Head C.G. Rotational Velocity

Figure A-2. Full Frontal Soft Pulse with AARS (BDSK0372)

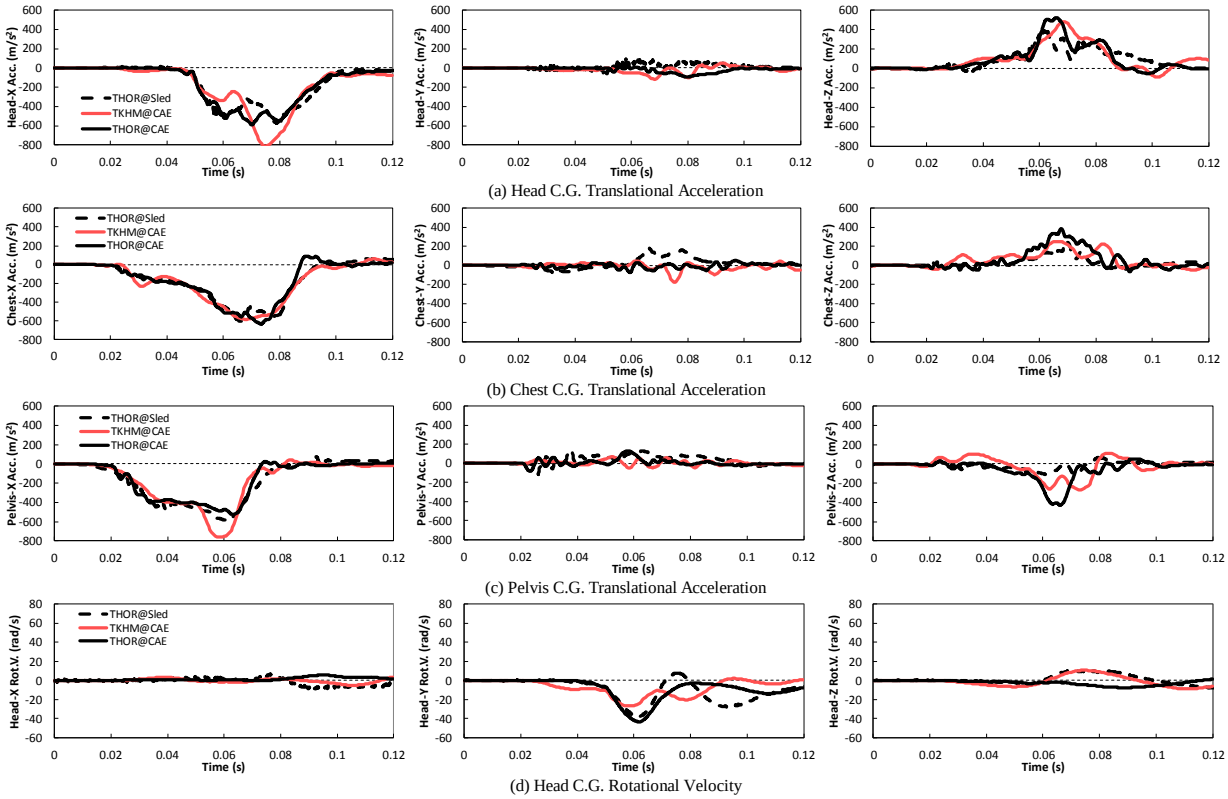

Figure A-3. Full Frontal Hard Pulse (BDSJ0179)

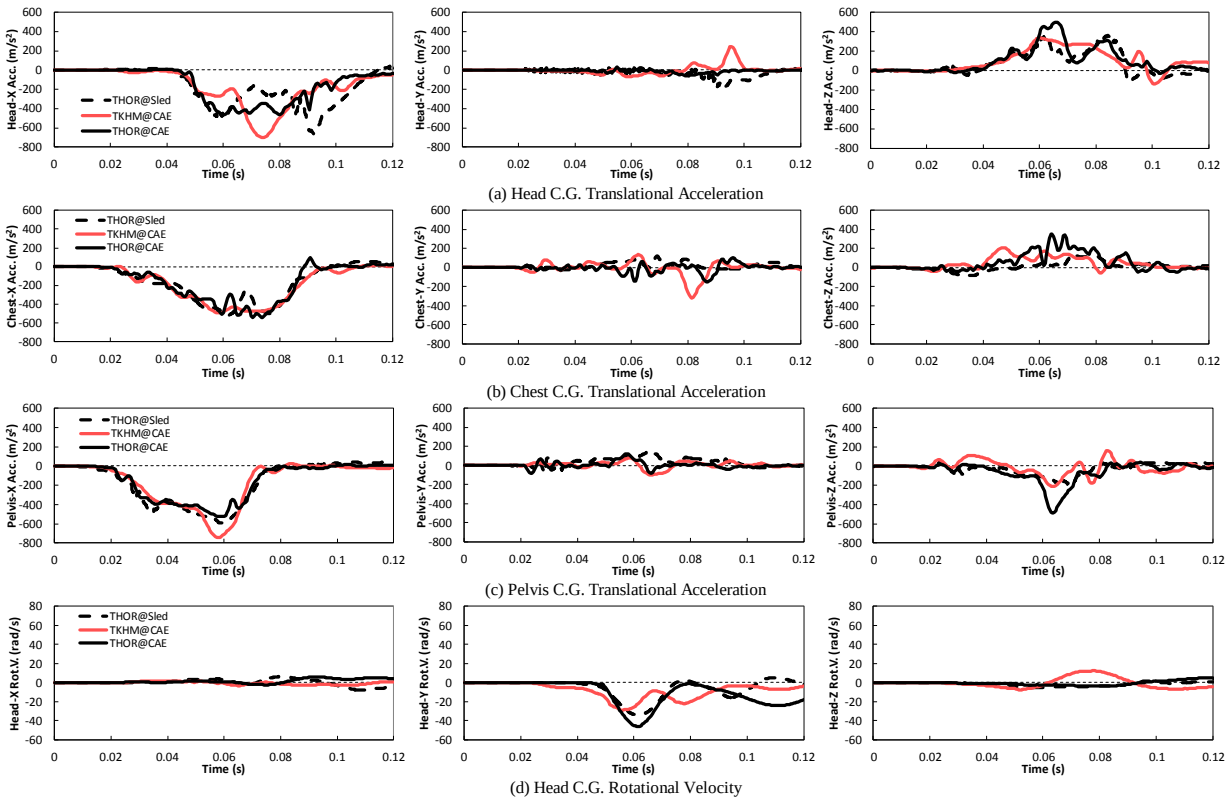

Figure A-4. Full Frontal Hard Pulse with AARS (BDSK0066)

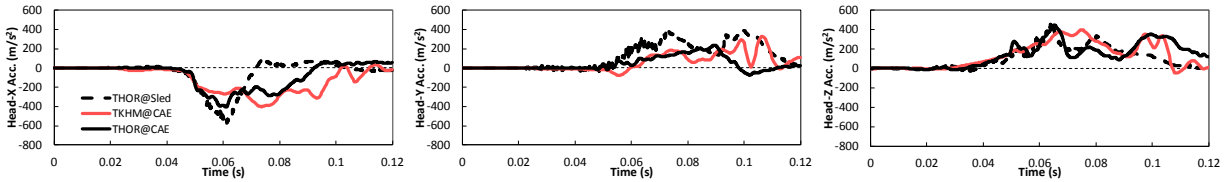

(a) Head C.G. Translational Acceleration

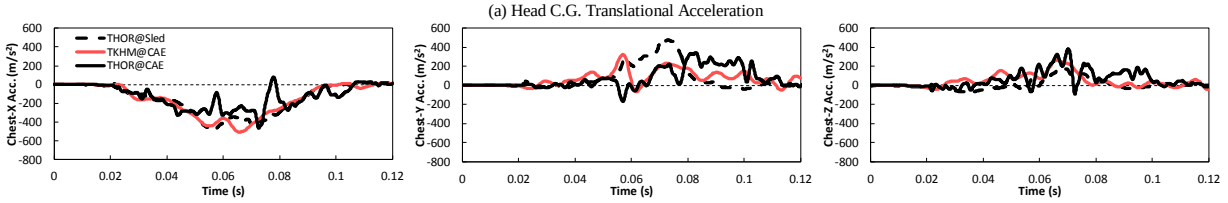

(b) Chest C.G. Translational Acceleration

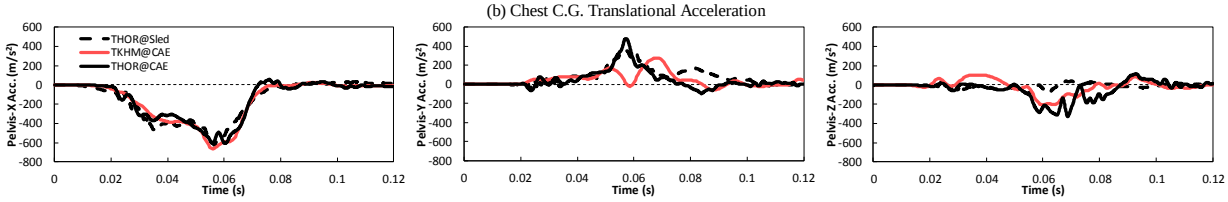

(c) Pelvis C.G. Translational Acceleration

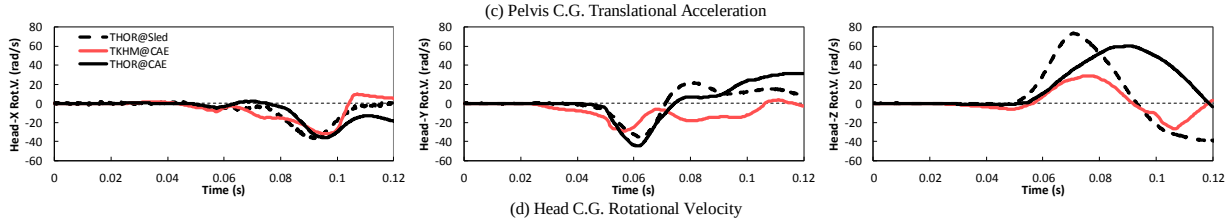

(d) Head C.G. Rotational Velocity

Figure A-5. Full Frontal Hard Pulse with AARS (BDSK0108)

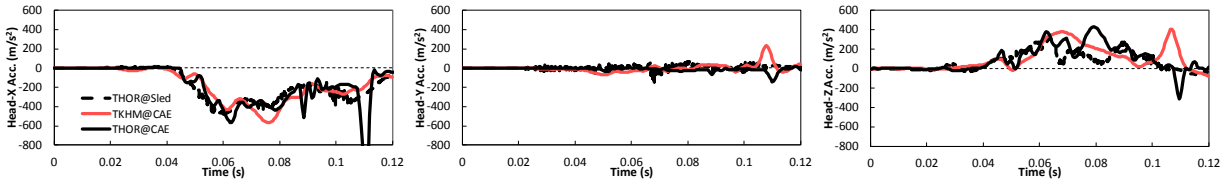

(a) Head C.G. Translational Acceleration

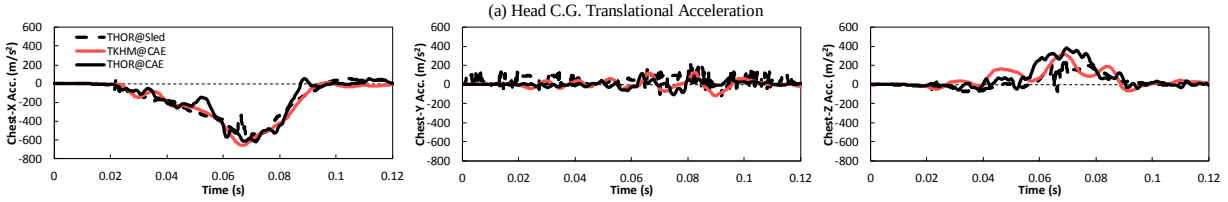

(b) Chest C.G. Translational Acceleration

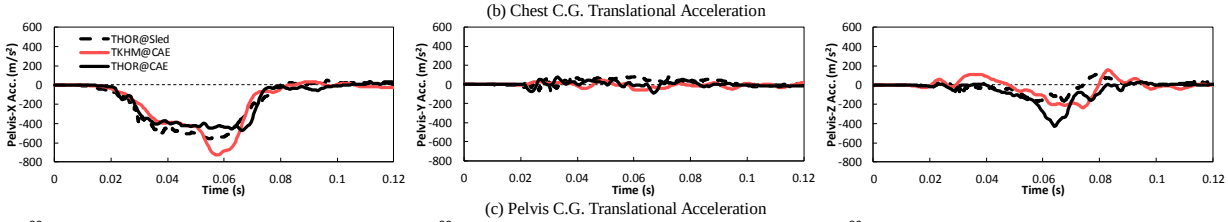

(c) Pelvis C.G. Translational Acceleration

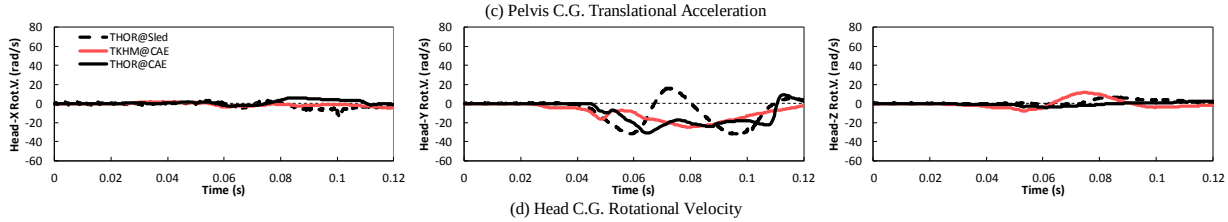

(d) Head C.G. Rotational Velocity

Figure A-6. Full Frontal Hard Pulse with AARS (BDSK0297)

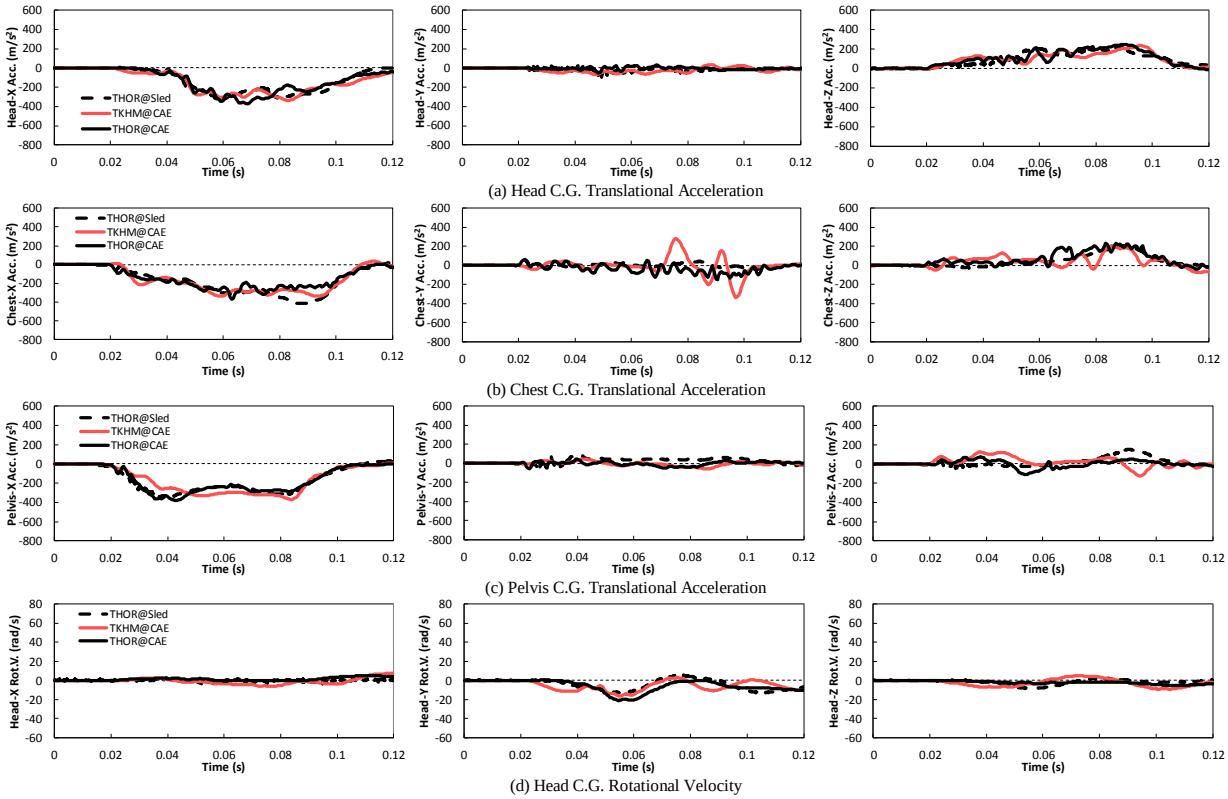

Figure A-7 Full Frontal Soft Pulse in Forward Position (BDSJ0173)

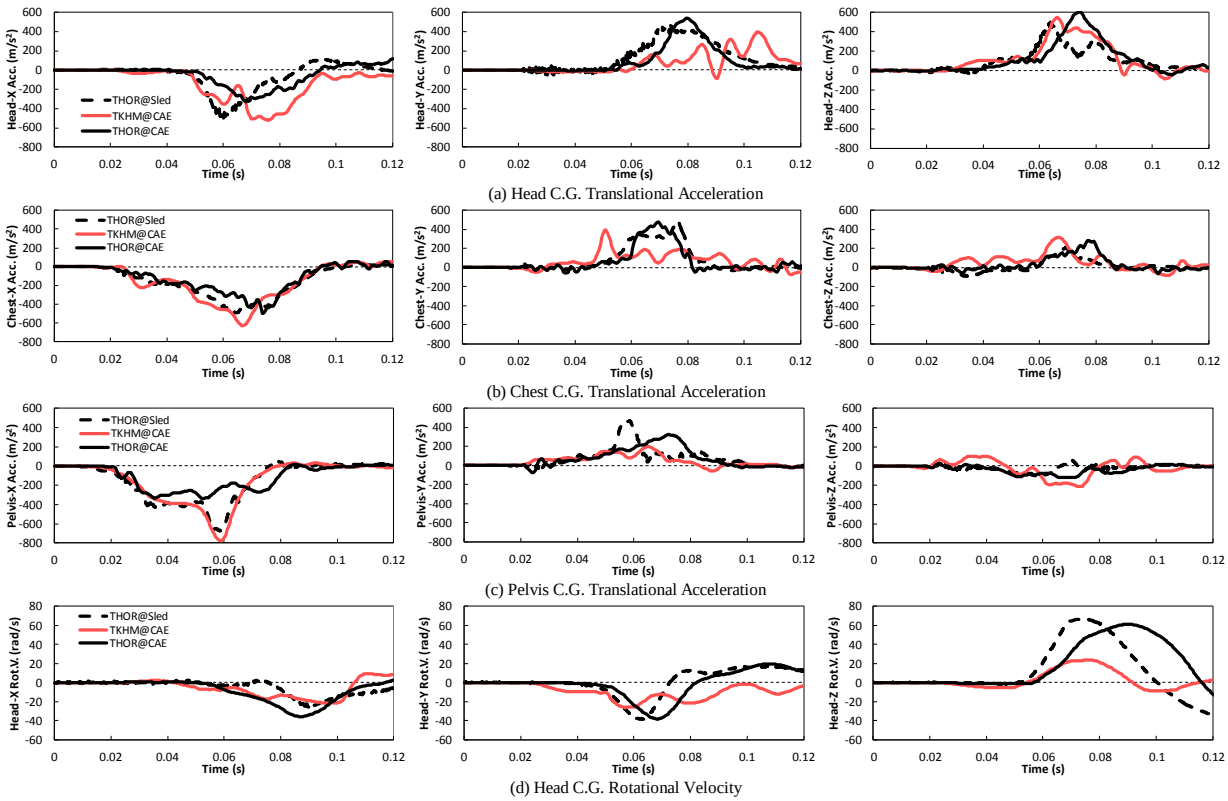

Figure A-8. Oblique Hard Pulse (BDSJ0180)

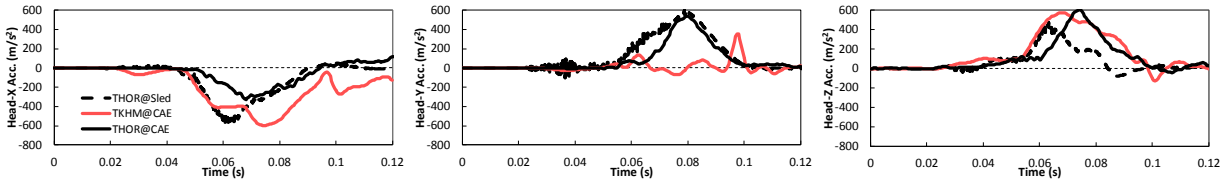

(a) Head C.G. Translational Acceleration

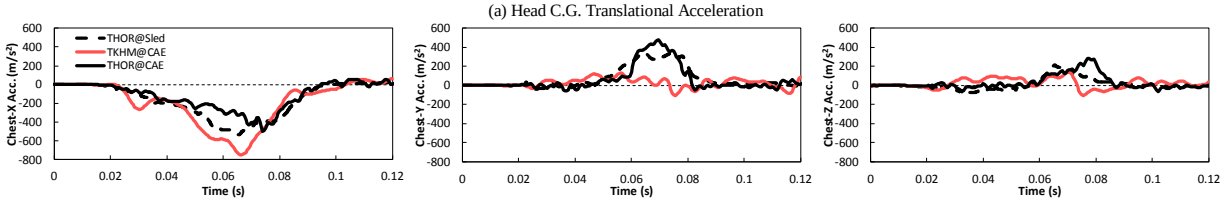

(b) Chest C.G. Translational Acceleration

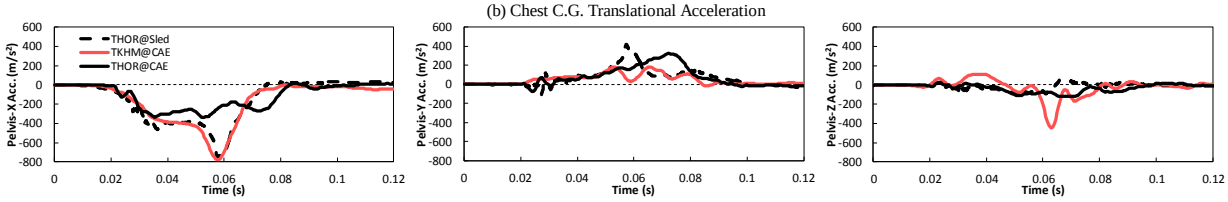

(c) Pelvis C.G. Translational Acceleration

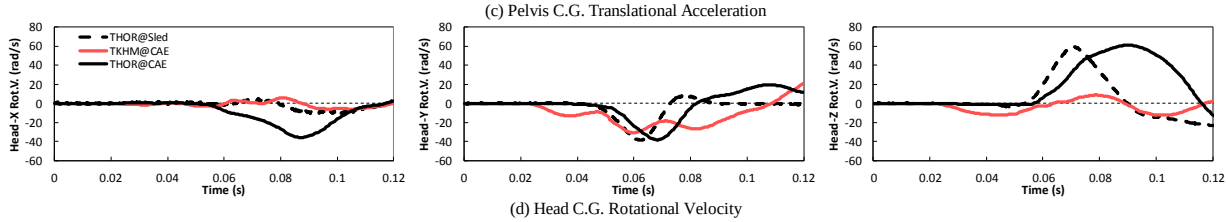

(d) Head C.G. Rotational Velocity

Figure A-9. Oblique Hard Pulse with AARS (BDSK0109)

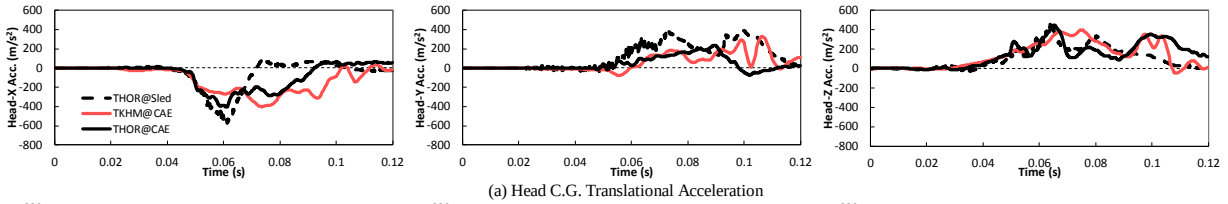

(a) Head C.G. Translational Acceleration

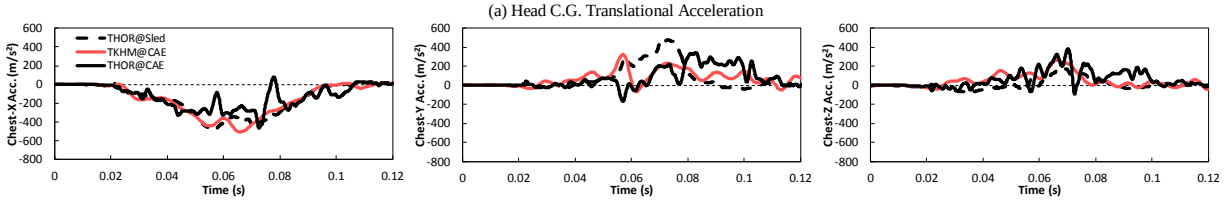

(b) Chest C.G. Translational Acceleration

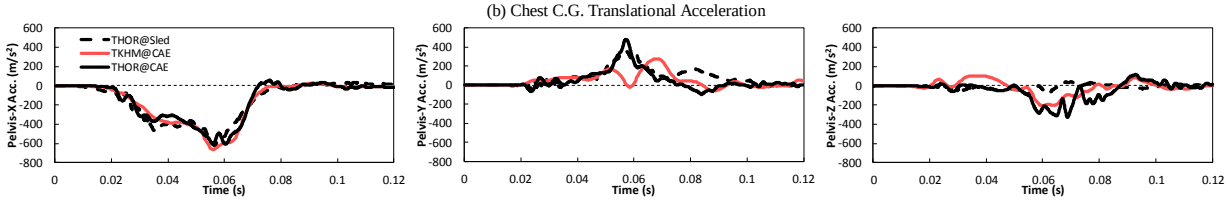

(c) Pelvis C.G. Translational Acceleration

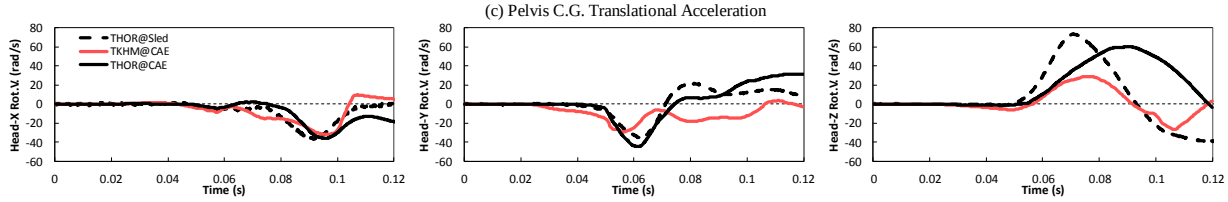

(d) Head C.G. Rotational Velocity

Figure A-10. Oblique Hard Pulse with AARS (BDSK0124)

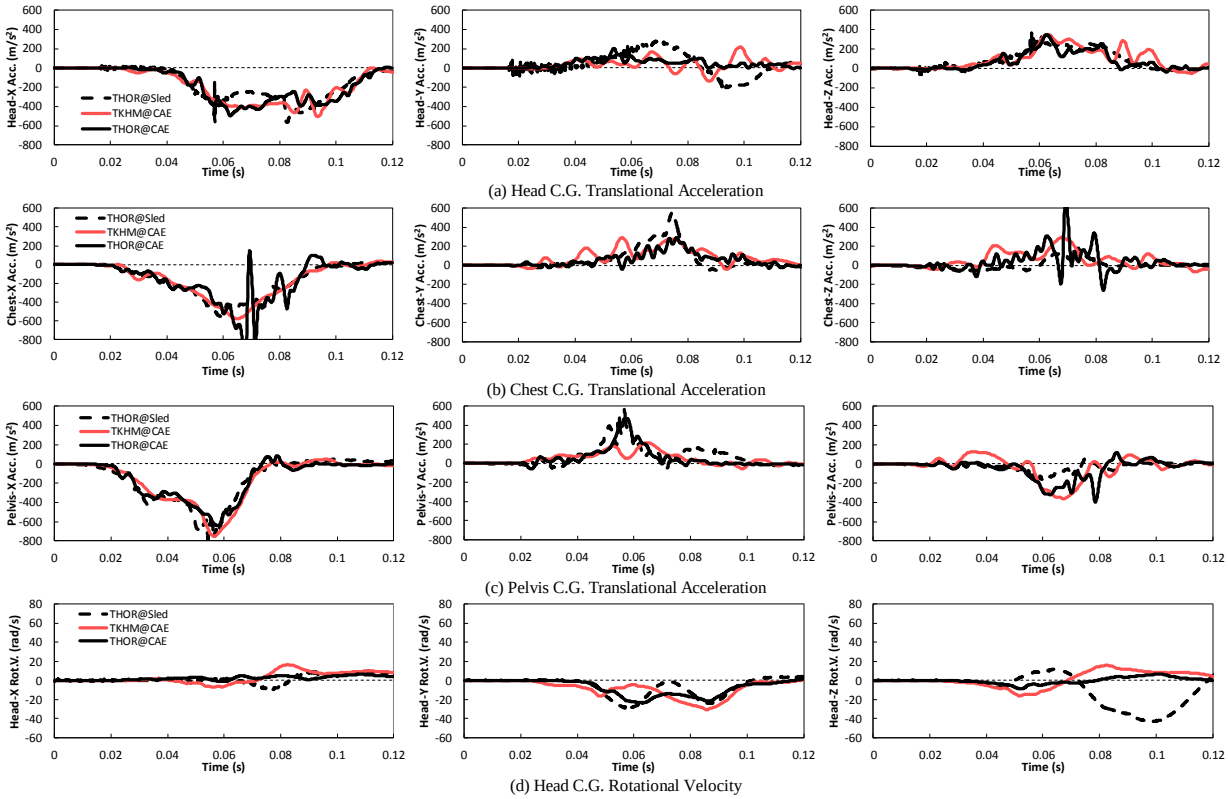

Figure A-11. Oblique Hard Pulse with AARS (BDSK0341)

APPENDIX B: TKHM v.5.3 Validations

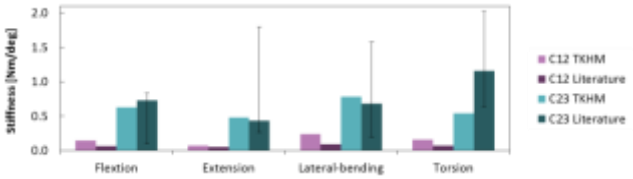

Figure B-1. Validation Results against Cervical Vertebra Tests

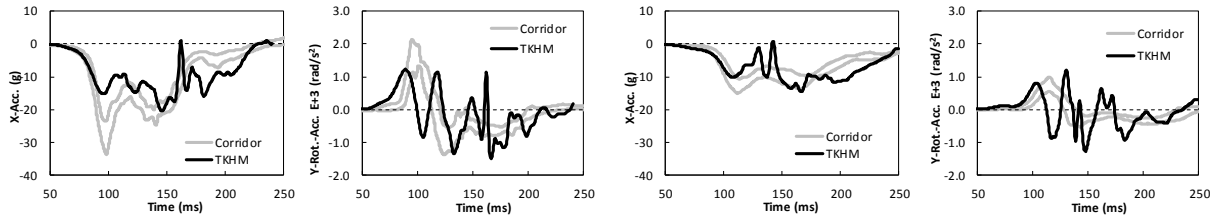

(a) NBDL Frontal 15G

(b) NBDL Frontal 8G

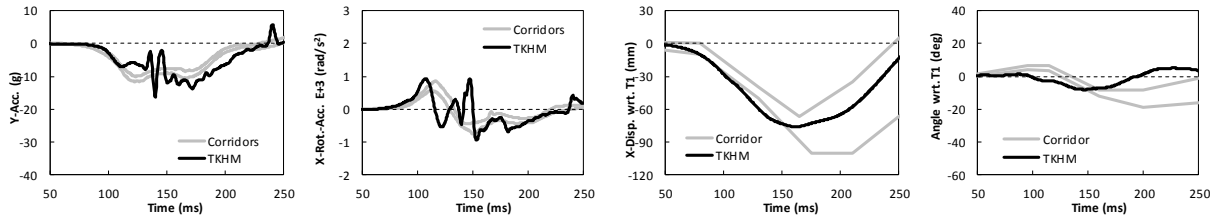

(c) NBDL Lateral 7G

(d) Davidsson Rear 4G

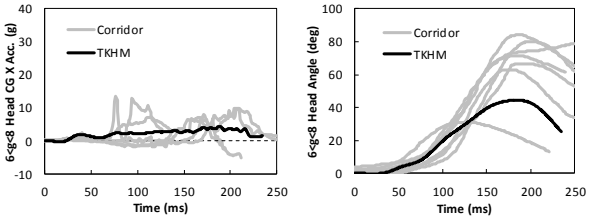

(e) Deng Rear 7G

Figure B-2. Validation Results against Head-Neck Component Tests

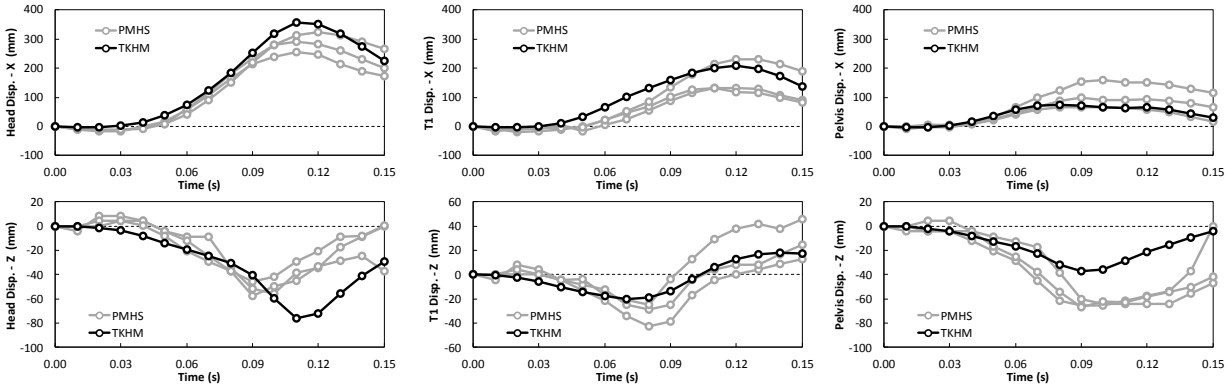

(a) Head C.G

(b) T1 C.G

(c) Pelvis C.G

Figure B-3. Validation Results against UVA PMHS Sled Tests